

EXPERIMENTAL STUDY OF FORMING LIMITS IN MULTISTAGE DEFORMATION PROCESSES

M.P. Sklad^①, E.H. Atzema^②, F.J. Schouten^②, M. de Bruine^② and A. Emrich^③

^① Corus Research Development & Technology
PO Box 10000, 1970 CA IJmuiden, The Netherlands,
on research leave from
the Dept. of Mechanical Engineering,
McMaster University,
Hamilton, Ontario, L8S 4L7, Canada
e-mail: sklad@mcmaster.ca

^② Corus Research Development & Technology,
PO Box 10000, 1970 CA IJmuiden, The Netherlands
e-mail: eiisso.atzema@corusgroup.com, frank.schouten@corusgroup.com, menno.de-bruine@corusgroup.com

^③ Adam Opel AG,
ITEZ MEP-Adv. Eng.&Simul./ 3D Anal.+VR
D-65423 Rüsselsheim, Germany
e-mail: albert.emrich@de.opel.com

Keywords: Multistage process, Forming Limit Stress Diagram, Forming Limit Diagram.

ABSTRACT. *The experimental study of forming limits in sheet material undergoing a multistage deformation process is presented. The study utilizes pre-strained samples, extracted from production parts, exhibiting a variety of deformation paths and strain magnitude, which are otherwise not available using traditional laboratory procedures. The effect on the forming limit of pre-straining magnitude and the direction relative to the material axis is examined with respect to subsequent deformation. The experimental data are applied to corroborate the validity of the forming limit stress diagram and the traditional forming limit diagram in the context of a multistage deformation.*

1. INTRODUCTION

With very few exceptions sheet metal parts are produced in multi-stage processes, in which the final shape of the part is formed from the initial blank in a series of separate operations of plastic deformation. In the multi-stage forming process, each operation is subject to the constraints of material formability limits. According to ISO standard 12004[1], the formability of sheet metal is represented by the forming limit curve, FLC, which expresses the forming limits of the sheet material in terms of a maximum allowable value of two principal strains, attained under conditions of proportional deformation. The FLC is plotted in a major-minor strain diagram referred to as the forming limit diagram, FLD. As in a multi-stage process each stage may involve a different strain path and/or a different orientation of the principal directions of deformation, the condition of proportional deformation is, in general, not maintained and therefore the conventional FLD may not be applicable.

At the present time there is no established method for evaluating the forming severity in multistage processes. One of the fundamental issues in the analysis of deformation in multistage processes is the ambiguity of the traditional forming limit diagram when applied to a multistage deformation because, in general, the principal strains are not additive. A concept referred to as the forming limit stress diagram, FLSD, shown in figure 1, also called the stress forming limit diagram, SFLD, [2][3][4][5], provides a solution to the ambiguity of the FLD and pledges to capture the dependence of the forming limits on the deformation history.

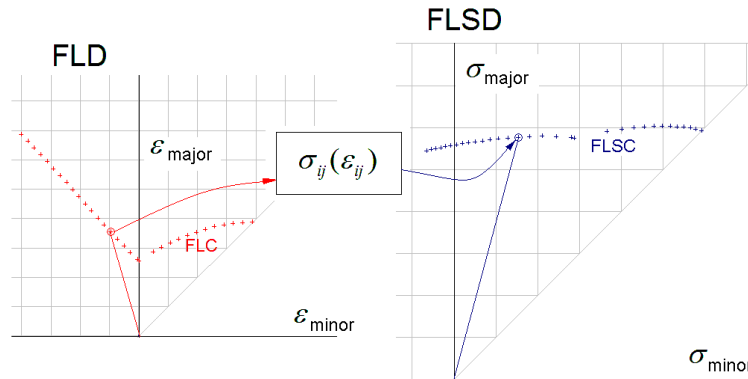


Fig. 1 Translation of FLD into FLSD for proportional deformation

The FLSD expresses the deformation state using the major-minor stress space instead of the major-minor strain space and employs the constitutive relationship, $\sigma_{ij}(\epsilon_{ij})$, of the material for translating the FLC into the forming limit stress curve, FLSC. The results presented in the works cited here, indicate that the shape of the FLSC remains unchanged in the case of a multistage process. This conclusion was also provided by Wu et al [6] based on a crystal plasticity numerical model, albeit without experimental verification.

The domain size of the deformation parameters characterizing forming limits in a multistage process increases rapidly with the number of process stages. In the case of experimental analysis of forming limits in multistage processes for specific materials and constant thermo-dynamic conditions during the experiment, the deformation forming limits at each stage can be characterized as a function of three distinct groups of process parameters: A - pre-strain magnitude, B - deformation path sequence and C - principal directions of deformation relative to the material configuration. The possible combinations of the interaction between these three groups are shown in figure 2, where the triple intersection

region, ABC, represents the forming limits in a general multistage process application, and the remaining regions provide a frame for separating the effects of different process parameters on forming limits during the research and analysis phase of the problem. In this framework, the region B encompasses the conventional FLD for a single stage proportional deformation process.

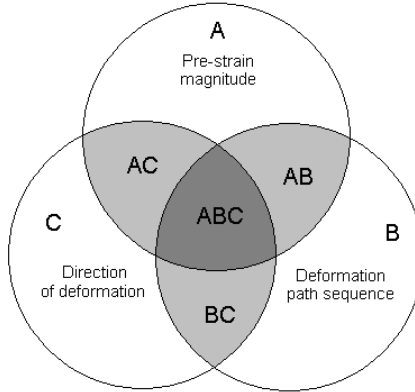


Fig. 2 Multistage process parameters affecting forming limits

With reference to figure 2, all cited works [2-5] explored the AB intersection region of the process parameters domain for a two stage process. The reported combinations of the processes parameters and their range are sparse due to difficulties in obtaining laboratory material samples uniformly pre-strained along different straining paths, with sufficient size to apply standard FLC procedures. In those works three pre-straining paths were applied: balanced bi-axial tension, plane strain, and uniaxial tension. The issue of material orientation, domains AC and BC in figure 2, was circumvented by maintaining the same principal directions of deformation for both stages with the principal strain directions aligned along the rolling and transverse directions of the sheet. Such an alignment simplifies the strain measurements and the calculation of strains and stresses. However, this simplification narrows the scope of the experimental evidence and raises uncertainty regarding the generalization of the constant FLSD [7]; firstly because material parameters and hence formability may vary with direction and secondly such an alignment is not usually attainable in industrial multistage process applications.

The overall objective of our work is the development of a technique to experimentally assess sheet forming severity in multistage processes, capable of covering a broad range of deformation paths and sequences along different orientation of deformation relative to the given material configuration. Furthermore the technique is applied to verify the validity of constant FLSC for different combinations of pre-straining deformation directionality on one specific material used in automotive body forming applications. At the onset of this work the following issues have been identified as significant: i) the proper measuring of the deformation in a multistage process, ii) ambiguity of the conventional FLD, iii) inclusion of changes of deformation directionality in the analysis of formability.

2. MATERIAL

The material selected for this study was Corus steel DX54D+Z (designation according to EN 10327). This is a galvanized (i.e. hot-dip zinc coated) steel for forming. The mechanical

properties of the steel used are listed in table 1. The material, being a forming steel, has high elongation and thus ductile behaviour. It also shows strong normal anisotropy accompanied by some planar anisotropy indicating good deepdrawability, albeit with some earing.

Table 1 – Mechanical properties of the test material

Thickness [mm]	direction [deg]	Rp [MPa]	Rm [MPa]	A80 [%]	r	n
0.815	0	163	297	46.0	2.171	0.226
	45	172	304	43.8	1.849	0.215
	90	169	293	47.4	2.575	0.220

In order to judge the applicability of the FLC to multi stage operations, the FLC first of all has to be measured. The FLC was measured before the current ISO norm was implemented at Corus and consequently it was measured using the internal Corus RD&T procedure AUT-STN-002 (which conforms to the old ISO 12004). More information on this can be found in [8]. Suffice to say that in implementing the draft ISO-norm for FLC (prEN ISO 12004-2) the results were checked against the previous results obtained by procedure AUT-STN-002 and were found to be equal within the accuracy of the test. Additional to the procedure, which demands only transverse direction (TD) measurements, three points were measured with major strain in rolling direction (RD). Both RD and TD results are plotted in figure 3. For comparison, figure 3 also includes a FLC generated using the Keeler-Brazier formula [9] for thickness 0.815mm and the average n-value of 0.219.

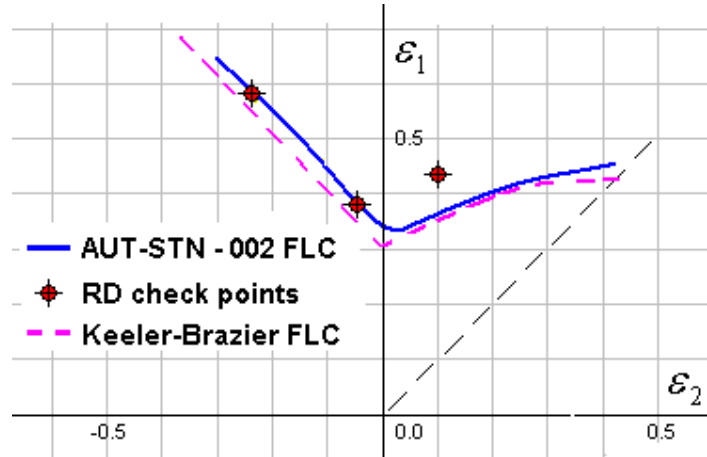


Fig. 3 FLC curves plus FLC RD check points

3. EXPERIMENTAL PROCEDURE

The deformation sequences leading to material failure that can be produced in the laboratory are very limited as compared to the almost unlimited possibilities occurring during actual production. For that reason, in this work, production parts were considered as the source of a pre-strained material with the expectation that samples extracted from production parts would exhibit a range of realistic deformation history.

3.1. Phase 1 – Development of analysis tools and a testing procedure

The experimental work on forming limits in multistage processes started with extracting coupons of a (assumed proportionally) pre-strained material and determining the mode and the magnitude of the pre-strain state, using strain grid analysis. These coupons were then subjected to a subsequent deformation causing failure and the parameters of the deformation sequence leading to that failure were determined. Out of several different testing procedures used to determine sheet metal formability, the Nakazima 75 mm diameter dome test was selected as the most suitable for bringing a pre-strained material to a state of failure. The non-ISO standard compliant 75mm Nakazima dome test tooling enabled usage of relatively large samples needed for maintaining a proportional deformation during the second stage of the process sequence. The undeformed material was etched with a 2.0 mm polka dot grid for strain measurements. In order to obtain the deformation history leading to failure; the deformation at the same material failure point has to be measured twice, after the first (safe) stage and after the second (failure) stage of the process. However, as in the multistage process the location of the failure is not known upfront when the first stage is recorded, the pre-strain measurements have to cover a larger area around the anticipated location of material failure. In this work the criterion for selecting the pre-strained regions of interest was by considering the near uniform distribution of the deformation over an area sufficient to accommodate the Nakazima sample. An efficient procedure for identifying such patches of near constant strains on the part surface is provided by the 3D grid measurement system- PHAST™ [10].

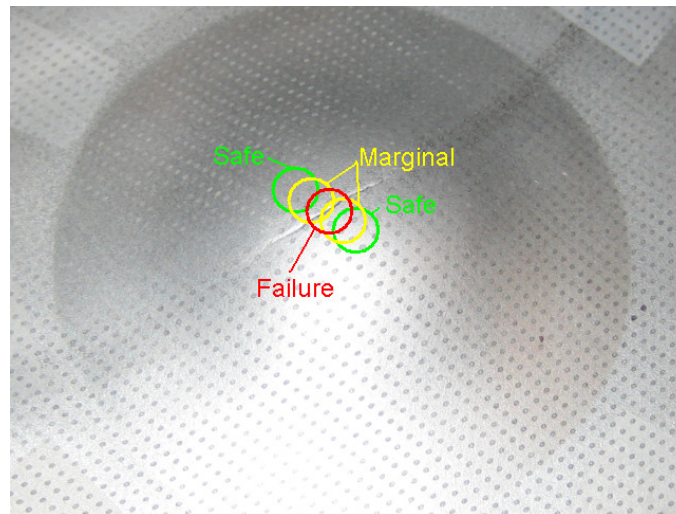


Fig. 4 Location of measured grid elements in the failure zone

The critical deformation in the second stage was measured using a grid analyzer at three or five different grid elements as shown in figure 4 according to the following convention. The first grid element labeled “failure” was located at the centre of the fracture line. Two grid elements adjacent to the “failure” element in a direction away from the fracture line were labeled “marginal” and occasionally the next two elements on both sides of the fracture line were measured and labeled “safe”. The measurements of the fractured element “failure” were done using a grid stitching function shown in figure 5. The grid stitching function removes the fracture gap running through the grid element before the strain measurements are performed on the digital image of the grid.

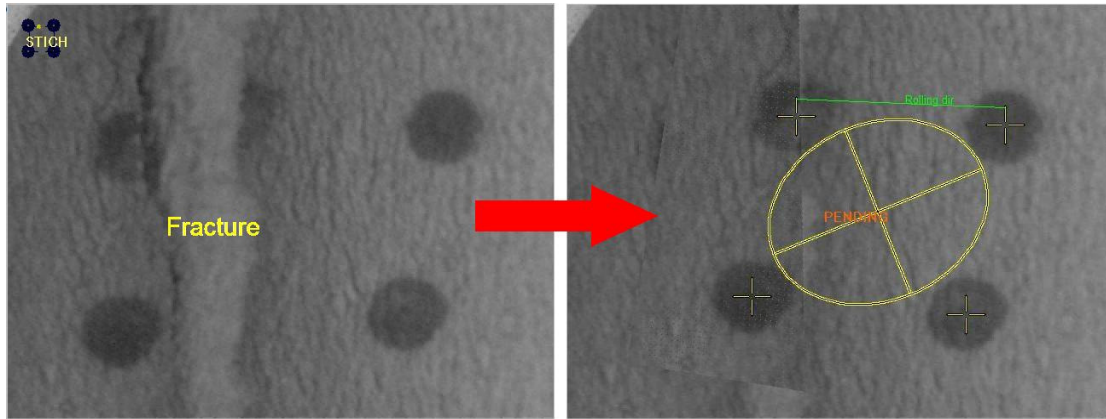


Fig. 5 Grid stitching provided by FMTI grid analyzer

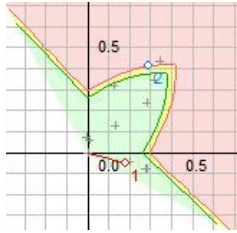
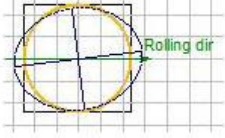
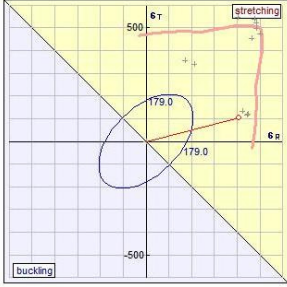
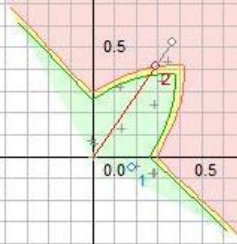
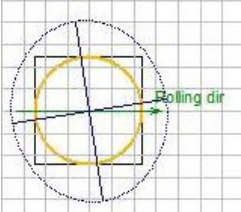
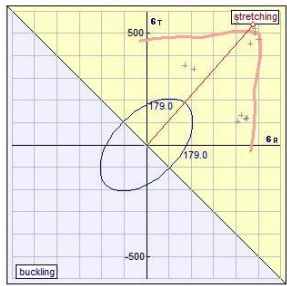
The issues of directionality of deformation with reference to the material coordinates have been addressed by replacing the conventional FLD diagram utilizing major and minor strains, $\varepsilon_{\text{major}} - \varepsilon_{\text{minor}}$, with a bi-directional diagram introduced by Lankford [11]. Lankford associated the principal strains and the points on the FLC with their proximity to the rolling, R, and transverse, T, directions of the sheet, $\varepsilon_{\text{R}} - \varepsilon_{\text{T}}$. A similar diagram was also used by Marciniak and Duncan for schematically depicting the fracture limits of the sheet [12]. It should be noted that even the bi-directional FLD is not entirely free of ambiguities as there are two points of discontinuity in the definition of the proximity to R and T directions of the sheet at the angle of $\pm 45^\circ$ to the rolling direction.

In this work the ambiguity of the conventional FLD in the context of multistage deformation has been resolved by treating and presenting deformation as a distinct and separate entity for each stage. This is consistent with the fact that in a multistage process the material is indeed relaxed at the completion of one operation, transferred to the next die and subjected to the next operation which induces new deformation which, in general, differs from the preceding one. The evolution of deformation in a multistage process is determined by several concurrent parameters:

- principal strains induced at a given stage,
- principal stresses associated with the principal strains,
- direction of the deformation with reference to the material,
- work hardening,

which are unique for each stage and ultimately lead to the failure of the material when the forming limit is reached. Table 2 shows a set of graphs depicting the essential process parameters, which was recorded for a two stage process terminated by material fracture. In table 2 the second and the last columns provide FLD and FLSD plotted in bi-directional coordinates. The third column provides circle grid analysis (CGA) interpretation of recorded strain increments. A complete description of the deformation requires a concurrent viewing the cluster of graphs presented in table 2. The example of a two stage process shown in table 2 generated by the grid analyzer for a model material consists of uniaxial tension in a direction 8 degrees away from the rolling direction during the first stage, followed by an (unbalanced) biaxial tension with major strain increment in a direction about -81 degrees to the rolling direction during the second stage. The strains and stresses are provided by the FLD and FLSD diagrams plotted using the Lankford material reference directions with an R and T convention. For reference, the FLD and FLSD graphs in table 2 also include the forming limit curves, FLC and FLSC.

Table 2 – Example of depicting deformation parameters for a two stage process

		Pre-strain stage			
Grid 1					
	$\Delta\bar{\epsilon}$	$\Delta\epsilon_1$	$\Delta\epsilon_2$	$\alpha_{\epsilon 1}$	$\Sigma\bar{\epsilon} -$
	0.19	0.18	-0.05	8	
		Failure stage			
Grid 1					
	$\Delta\bar{\epsilon}$	$\Delta\epsilon_1$	$\Delta\epsilon_2$	$\alpha_{\epsilon 1}$	$\Sigma\bar{\epsilon} -$
	0.70	0.41	0.29	-81	0.90

3.2. Phase 2 – Attaining experimental forming limit data for a range of two stage process parameters

During the second stage the testing method was applied to generate a matrix of experimental data for a specific material subjected to a different pre-straining in an industrial process. The source of the pre-strained material was a part, shown in figure 6, undergoing pre-production die tryout. During the die tryout a 2 mm polka dot grid was etched on the blanks at the locations of anticipated deformation. The etched grid was aligned with the rolling direction of the sheet. In order to obtain different levels of pre-strain three different settings of the clamping forces were applied and several parts were produced for each setting.



Fig. 6 Panel as formed

The preparation of the Nakazima test often required flattening of the extracted material, which resulted in the formation of buckles. The ridges of buckles were marked and, in case of a subsequent fracture close to the buckle, such samples were rejected for use in this study. Figure 7 shows Nakazima test samples with buckles before and after the second stage deformation.

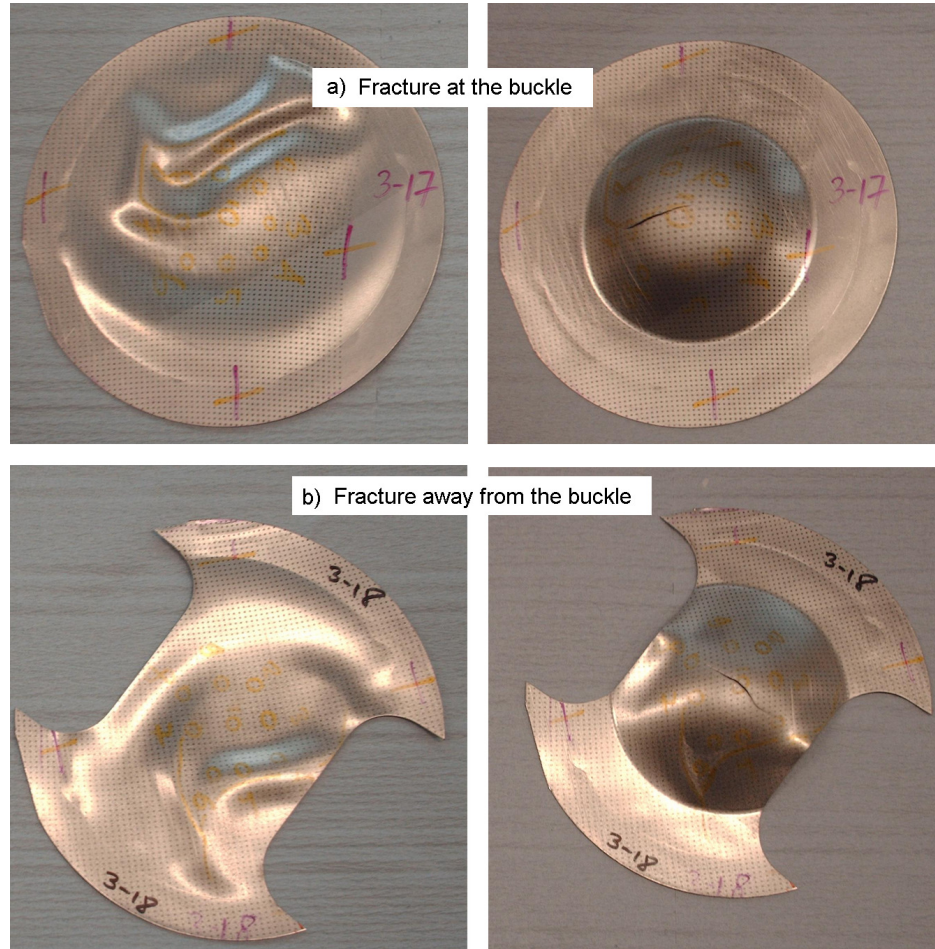


Fig. 7 Samples with buckles: a) rejected, b) accepted

4. RESULTS

The part provided a range of different pre-straining paths, distributed between the uniaxial tension mode and the biaxial tension mode in the principal strain space. While changes of the clamping force had a noticeable effect on the magnitude of the pre-strain, the mode and directionality were essentially set by the part geometry and were not affected by the clamping force. This limited the available pre-strain mode and directionality to those listed in table 3. According to table 3 the direction of ε_1 indicates that the deformation process on the left side of the part in figure 6 was dominated by stretching which occurred in the transverse direction to the sheet, because open ended spare housing reduced tension in the rolling direction. The corner areas on the right side of the part in figure 6 were stretched in the diagonal direction of the sheet.

Table 3 – Example of pre-strain state (part #3)

Area	1	2	3	4	10	11	14	15	16	17	18	33	35	44	45
Mode															
UT	X	X	X	X								X		X	
UT-PS					X		X	X							
PS						X				X	X				
PS-B									X				X		X
Approx. $\bar{\epsilon}$	0.15	0.2	0.18	0.15	0.3	0.2	0.25	0.2	0.1	0.25	0.15	0.1	0.15	0.1	0.15
Approx. dir ϵ_1	-72	-76	76	76	-71	-79	-84	85	-50	-82	-90	45	65	-45	84

Mode: UT – uniaxial tension, PS – plane strain, B –biaxial tension

While the directionally and the deformation mode were predetermined for the pre-strained material, there were no constraints on the straining modes in the Nakazima test planned for the second deformation stage. However, in order to capture the major trends with the limited number of pre-strained samples, the deformation induced in the second stage, aimed at the three most basic straining paths in terms of the FLC: equi-biaxial tension (B), plane strain (PS) and uniaxial tension (UT). Furthermore, all samples within each of these three categories, B, PS and UT, had the same geometry but varied in the pre-strain mode, the pre-strain magnitude and the orientation. The three geometries used were 165 mm circles for the equi-biaxial tension and 85 mm and 45 mm “dog bone” width samples for the plane strain and the uniaxial tension test respectively. As the orientation of the deformation on the pre-strained material was already non-collinear with 0, 45 and 90 degrees directionality of the sheet, the “dog bone” samples were made with the approximate orientation of the shaft section of 0, 45 and 90 degrees to the direction of major strain, ϵ_1 , as determined for the pre-strained state rather than to the traditionally used rolling direction of the sheet. This was done intentionally to explicitly address the effect of changing the directionality of deformation on formability.

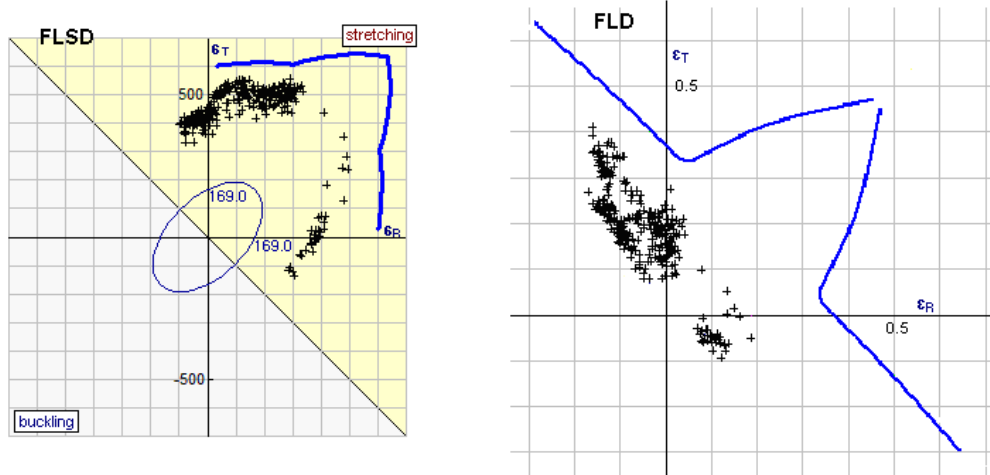


Fig. 8 Forming limits and pre-stain data points collected from all samples

The experimental FLSD and FLD and pre-strain data for all measured samples consisting of about 400 points are shown in figure 8. The FLSD data points were calculated from FLD using average values of material constants listed in table 1. The lumped groups of points in figure 8 indicate preferred areas with relatively constant strains; however the less preferred areas exhibiting more noticeable pre-strain gradients were also used in this study. It should be noted that the part provided an extensive number of samples pre-strained under near uniaxial and near plane strain tension but only a few samples subjected to balance biaxial tension in the stretching zone of FLSD and no samples in the buckling and shear zone of the FLSD. The

few samples pre-strained under balanced biaxial tension could not be considered due to a fracture occurring in the proximity a buckle as shown in figure 7a.

The matrix of samples demonstrating the effect of work hardening and the effect of strain directionality on the forming limit in the multistage process is shown in figure 9.

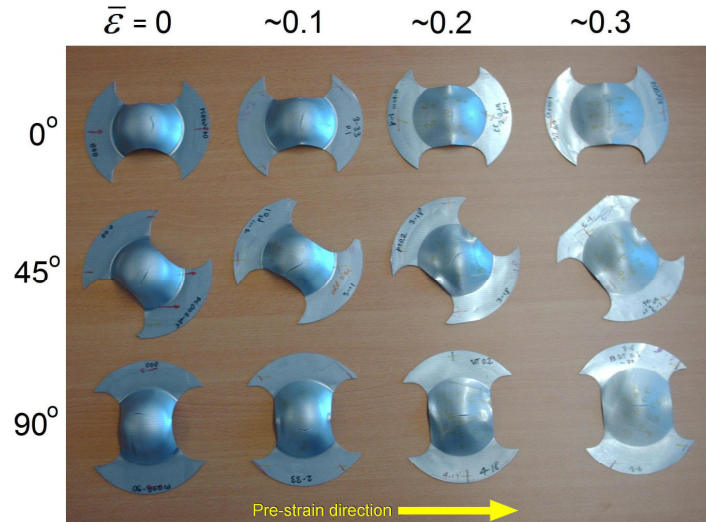


Fig.9 Matrix of samples produced by uniaxial tension pre-strain followed by fracture under plane strain tension.

The samples shown in figure 9 were obtained through the sequence of uniaxial tension followed by plane strain tension. All samples in figure 9 had the same initial geometry, with a shaft width of 85 mm, targeting the plane strain failure. The arrangement of samples in figure 9 is as follows: the columns correspond with the magnitude of the effective strain, $\bar{\epsilon}$, induced during the initial pre-strain; $\bar{\epsilon} = 0.0, 0.1, 0.2$ and 0.3 . With the exception of the first column pertaining to the undeformed material and R-D-T directions of the sheet, the rows are arranged according to the orientation of the major stretch under plane strain (second stage deformation), with reference to the major strain direction in the previously induced uniaxial tension. For clarity, the plane strain tension direction angles of 0, 45 and 90 degrees are also indicated by the angular orientation of the samples in each row. Comparison of the failure deformation measured for samples in each column shows no effect of orientation on formability for the material tested.

5. DISCUSSION

The matrix of samples in figure 9 shows that, as expected, the amount of pre-strain, indicated by the position in a row, has a very significant effect on the strains reached in the second stage – forming limit. On the other hand the effect of orientation, indicated by the difference between the samples in each column, is practically non-existent. The lack of effect of directionality of the pre-strain on the forming limit has also been confirmed for other available combinations of straining paths. Thus the material failure data were translated from the bi-directional stress space of the FLSD back to the proportional deformation strain space FLD, using the inverted constitutive relationship, $\epsilon_{ij}(\sigma_{ij})$, and employing the non-directional major-minor strain convention. The second stage deformation in stress and strain domains is shown in figure 10. The distribution of safe, marginal and fail points is consistent with the

forming limit curves in both stress and strain coordinates.

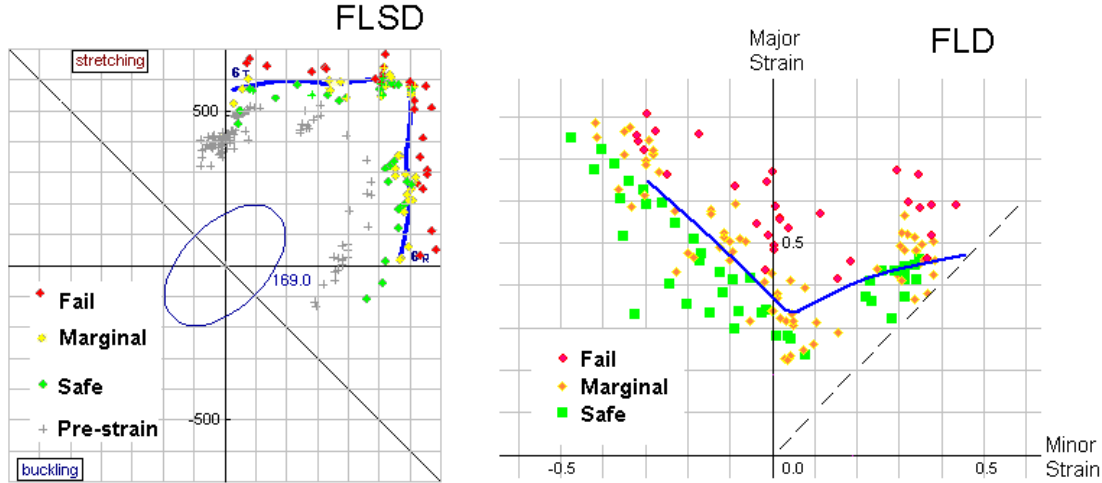


Fig. 10 FLSD and traditional FLD combining data for samples used in the second stage.

6. CONCLUSIONS

The procedure for measuring deformation in a multistage process has been established and applied to analyze formability in two stage processes.

The procedure takes into account the directionality of deformation with respect to the rolling direction of the material.

Samples extracted from production parts were used successfully with the Nakazima test to determine formability limits within a broad range of pre-strain deformation not available during conventional laboratory procedures.

The existence of the folds on the samples formed during flattening may significantly reduce formability.

The formability limits determined for the tested combinations of deformation stages are consistent with the stress space based forming limit curve, FLSC.

The experimental results show no effect of the deformation directionality on forming limits for steel DX54D+Z in the multistage deformation process.

All fractured samples produced during the course of this project exhibited a localized necking failure mode. With hindsight, this is probably to be expected for a forming grade steel.

7. FURTHER RESEARCH / RECOMMENDATIONS

It is recommended to repeat the research using other materials that behave in a less ductile manner, (e.g. current (A)HSS grades) to see whether the conclusions hold for those materials as well. These materials may show a different failure behaviour. Certain strain paths, for instance, may lead to shear fracture whereas others may lead to failure by necking. In this work the first stage consisting of plane strain and uniaxial tension followed by three basic modes of final strain were tested. Secondly it is recommended to test the biaxial and compression causing thickening of the sheet pre-strain modes. Adding these other sequences would complete the picture.

8. ACKNOWLEDGEMENTS

The authors would like to thank the management of Corus and GME and GM-US for their support in this collaborative project.

9. REFERENCES

1. "Metallic materials - Guidelines for the determination of forming-limit diagrams", *ISO Standard 12004-2*.
2. R. Arrieux, C. Bedrin, M. Boivin, "Determination of an intrinsic forming limit stress diagram for isotropic sheets", *Proc 12th IDDRG Congress*, Sta, Margherita Lige, 1982, 61-71.
3. L. Zhao, R. Sowerby, M.P. Sklad, "A theoretical and experimental investigation of limit strains in sheet metal forming", *Int. J. Mech. Sci.*, 1996, 38, 1307-17
4. T.B. Stoughton, "A general forming limit criterion for sheet metal forming" *Int. J. Mech. Sci.*, 2000, 42-1, 1-27.
5. A. Graf, W.F. Hosford, "The influence of strain path changes on forming limit diagrams of AL 6111-T4", *Int. J. Mech. Sci.*, 1994, 36, 897-910.
6. P.D. Wu, A. Graf, S.R. MacEwen, D.J. Lloyd, M. Jain and K.W. Neale, "On forming limit stress diagram analysis", *Int. J. Solids and Structures*, 2005, 42-8, 2225-2241
7. K. Yoshida, T. Kuwabara, M. Kuroda, "Path-dependence of the forming limit stresses in a sheet metal", *Int. J. Plasticity*, 23-3, 2007, 361-384.
8. Eisso H. Atzema, Ardy Duwel, Louisa Elliott, Peter F. Neve, Henk Vegter, "Appreciation of the Determination of the Forming Limit Curve", *Numisheet 2002*, Jeju, Korea, 2002
9. S.P. Keeler, W.G. Brazier, "Relationship Between Laboratory Material Properties. and Press Shop Formability", *Proc Conf. Microalloy 75*, 1977, 517-528.
10. E.H. Atzema, The new trend in strain measurements: fast, accurate and portable: PHAST™, *SheMet 2003*, University of Ulster, Jordanstown, United Kingdom, eds. Singh, U.P.; Geiger, M.; Kals, H.J.J.; Shirvani, B.; 14-16 April 2003
11. W.T. Lankford, J.R. Low, and M. Gensamer, "The Plastic Flow of Aluminium Alloy Sheet Under Combined Loads", *Trans AIME*, 171, 1947, p. 574.
12. Z. Marciniak, J.L. Duncan, *Mechanics of Sheet Metal Forming*, 1992, London: Edward Arnold.